Electronic Structure, Molecular Electrostatic Potential, and NMR Chemical Shifts in Cucurbit[*n*]urils (*n* = 5−8), Ferrocene, and Their Complexes

Rahul V. Pinjari and Shridhar P. Gejji*

Department of Chemistry, University of Pune, Ganeshkhind, Pune 411007, India

Received: August 14, 2008; Revised Manuscript Received: September 30, 2008

Electronic structure and molecular electrostatic potential (MESP) in ferrocene (FC), cucurbit[*n*]urils (CB[*n*]) with *n* = 5−8, and their host−guest complexes are obtained within the framework of density functional theory. MESP topography that is employed to gauge the dimensions of the CB[*n*] cavity estimates that the cavity height increases from 7.25 to 7.70 Å along CB[*n*] homologue series, whereas the diameter of the CB[8] (8.57 Å) cavity is larger than twice that of CB[5] (3.91 Å). MESP investigations reveal deeper minima near ureido oxygens in CB[5] along with large electron-rich regions at its portal. A lateral interaction of the guest FC with hydrophilic exterior of the CB[*n*] portal and its encapsulation within hydrophobic cavity of the host are analyzed. The present calculations suggest that CB[5] does not yield stable complexes in either case. FC interacts laterally with CB[6], and inclusion of the guest occurs, both parallel as well as perpendicular to the CB[*n*] axis, in the cavity of higher homologue. Self-consistent reaction field studies indicate that, in the presence of water as a solvent, encapsulation of FC in parallel fashion is favored within CB[7] and CB[8] cavities. NMR chemical shifts (δ_H) of CB[*n*] protons remain practically unchanged with an increase in the cavity size; however, they are influenced significantly by water. The spectra thus obtained in aqueous solution agree with those observed experimentally. The δ_H values in FC−CB[*n*] complexes indicate deshielding of FC protons directed toward portals, while those pointing toward nitrogens exhibit up-shifts in the spectra.

Introduction

Cucurbit[*n*]urils, cyclic oligomers of glycouril denoted by CB[*n*] (*n* being the number of repeating glycouril units), are molecular containers that are capable of binding a variety of guest molecules within their cavities.[1] Interestingly, the X-ray crystal structure of CB[6] was unraveled only in 1981,[2] decades after its synthesis by condensation of glycouril and formaldehyde in acidic condition.[3] In the past 10 years, synthesis and characterization of CB[*n*], *n* = 5−8, homologues have been carried out[1,4,5] while the existence of higher CB[*n*] homologues has been confirmed through electrospray ionization mass spectroscopic experiments. CB[*n*] cavity composed of hydrophilic portals lined by ureido oxygens is capable of accommodating a variety of guests that include acids, alcohols,[6,7] peptides,[8,9] ferrocene, and cobaltocene,[10−15] as well as metal ions and their complexes.[1,16−21] Remarkably enough, the CB[*n*] hosts in fact bind some metals more strongly compared to what [18]crown[6] does.[22,23] These hosts essentially interact with a positively charged species which leads to enhanced solubility in concentrated aqueous acid.[22,24] The attributes such as high affinity, different cavity volumes, solubility in different solvents, selectivity, and controlled inclusion of different guests endow CB[*n*] derivatives with their versatility. They are utilized in separation technology,[25,26] supramolecular chemistry,[10,27−37] catalysis,[38−40] molecular recognition,[41,42] drug delivery vehicles,[14,18,43] DNA binding, gene transfection,[44,45] nanotechnology,[46,47] dendrimers,[15,48] molecular necklaces,[49−51] rotaxanes, and pseudorotaxanes.[40,52−61] CB[*n*] has been used in tunable molecular machines where the complexation can be turned on or off and the operational speed can be controlled by varying the pH.[62] By virtue of its large cavity size, CB[8] (or sometimes CB[7]) can form a termolecular complex accommodating two aromatic molecules simultaneously,[4] a feature that has been exploited in organic synthesis[63−69] and charge-transfer complexes.[36,70,71] In particular, CB[8] accelerates and controls the photoreaction between the guest molecules in ternary complexes, leading to a product with high stereoselectivity.[63] Ferrocene (FC) and violegen in CB[*n*] hosts are frequently used guests in a wide range of applications. Moreover, NMR spectroscopy has been used to understand encapsulation of viologen[72] and FC[73] at focal point functionality in newkome-type dendritic block.

On the theoretical front, ab intio and density functional calculations have been carried out to quantify stabilities of CB[*n*] and their methyl-substituted derivatives.[74] Electronic structure of CB[*n*][75] and their thio analogues[76] have also been derived. Recent work by Carlqvist and Maseras[77] on cycloaddition of azide and alkyne within the CB[6] cavity brings out its potential as a highly efficient supramolecular catalyst. Within the semiempirical framework,[78] interaction of transition-metal ion with thia-CB[*n*] has also been investigated. A supramolecular strategy for the synthesis of thia-cucurbituril nanotubes of a desired molecular length is proposed. A class of tubular nanostructure from thia-cucurbituril macrocycles with transition-metal ions has been designed. The frontier orbitals here indicate that the growth of nanotube is likely to initiate at one end. Furthermore, the NMR has widely been used to gain insights for the interaction of guest with CB[*n*] hosts. Theoretical calculations due to Buschmann et al.[79] have shown that the frontier orbitals in CB[*n*] homologues are similar and the predicted NMR chemical shifts therein turn out to be nearly unchanged.

Despite the important studies outlined above, almost no endeavor, be it ab initio or be it within DFT, appears to have been made toward description of inclusion of the guest

* Corresponding author. E-mail: spgejji@chem.unipune.ernet.in.

10.1021/jp807268v CCC: $40.75
Published on Web 11/14/2008

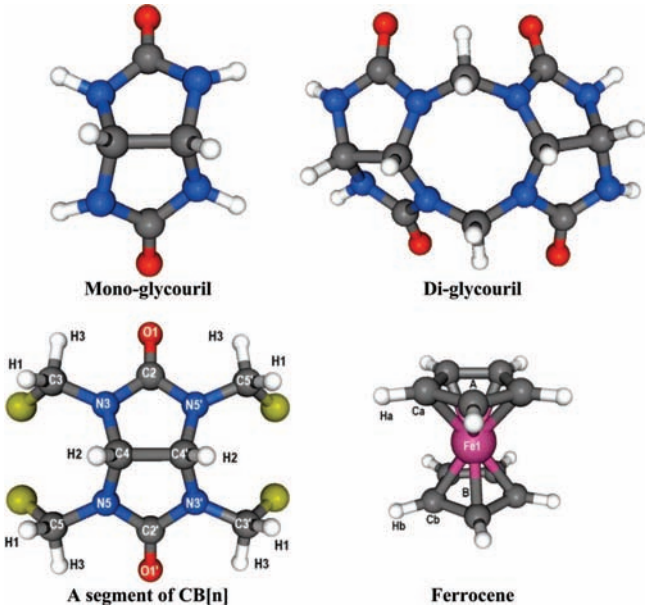

Figure 1. Optimized geometries of monoglycouril, diglycouril, and atom numbering scheme in CB[*n*] and ferrocene.

molecule(s) by CB[*n*] cavities. In pursuance of precisely this theme, we derive the electronic structure, molecular electrostatic potentials (MESP), and the NMR chemical shifts in CB[*n*], FC, and their complexes. Relative stabilizations of complexes with different binding modes of FC with CB[*n*] have also been analyzed.

Computational Method

Geometry optimization of CB[*n*] homologues and their complexes with FC was carried out employing the Gaussian 03 suit of programs[80] using the density functional theory incorporating Becke's three-parameter exchange augmented by Lee, Yang, and Parr's (B3LYP) correlation functional.[81,82] Internally stored 6-31G(d) basis was used in these calculations. The unit energy (E_{Unit}) was computed as a difference in energies of monoglycouril and diglycouril (cf. Figure 1).[74] The energy of stabilization of CB[*n*] homologues was estimated via $E_{\mathrm{Stabilz}} = E_{\mathrm{CB}[n]} - n * E_{\mathrm{Unit}}$ (i.e., subtracting n times the unit energy from that of the CB[*n*]).

The MESP at a spatial point r, $V(r)$, is given by

$$V(r) = \sum_{A=1}^{M} \frac{Z_{\mathrm{A}}}{|r - R_{\mathrm{A}}|} - \int \frac{\rho(r')d^3r'}{|r - r'|} \qquad (1)$$

where M is total number of nuclei in the molecule, Z_{A} defines the charge of the nucleus located at R_{A} and $\rho(r)$ is the electron density at location r. The two terms in V refer to the bare nuclear potential and the electronic contributions, respectively. Regions conducive to the electrophilic interactions are governed by substantial negative values of MESP. The topography in MESP

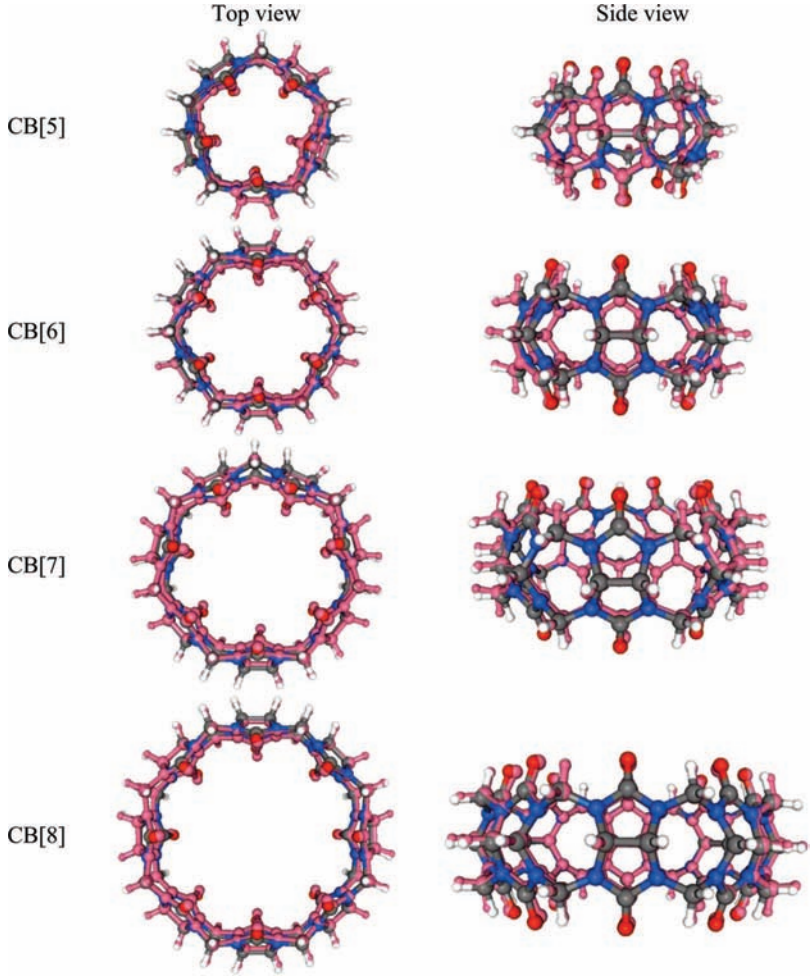

Figure 2. Top and side views of the B3LYP-optimized geometries of the CB[*n*] homologues superimposed with their crystal structures (displayed in pink).

TABLE 1: B3LYP-Optimized Bond Lengths (in Angstroms) and Bond Angles (in Degrees) in CB[*n*] Homologues

	CB[5]	CB[6]	CB[7]	CB[8]
O_1C_2	1.212	1.213	1.213	1.213
C_2N_3	1.393	1.392	1.393	1.393
N_3C_3	1.447	1.446	1.446	1.445
N_3C_4	1.447	1.446	1.446	1.446
C_4C_4'	1.575	1.572	1.570	1.568
C_3H_1	1.098	1.100	1.101	1.102
C_4H_2	1.100	1.101	1.102	1.102
C_3H_3	1.093	1.093	1.093	1.093
O−O	5.390	7.190	8.530	10.30[a]
O_1O_1*	3.330	3.596	3.800	3.942[c]
O_1H_3	2.425	2.403	2.392	2.387[b]
$O_1C_2N_3$	126.4	126.4	126.4	126.4
$C_2N_3C_3$	121.0	121.2	121.1	121
$C_2N_3C_4$	113.0	113.0	112.8	112.7
$N_3C_4C_4'$	103.3	103.4	103.4	103.5
$N_3C_2N_5'$	107.1	107.1	107.2	107.2
$C_3N_3C_4$	125.8	125.1	124.4	124
$N_3C_4N_5$	117.6	117.2	117.0	116.8
$O_1C_2N_3C_3$	3.4	−1.8	−5.3	−7.9
$O_1C_2N_5'C_5'$	−3.4	1.8	5.3	7.9
$O_1C_2N_3C_4$	−172.6	−172.3	−171.4	−171.0
$C_2N_3C_4N_5$	−115.9	−115.8	−116.5	−116.8
$C_2N_3C_4C_4'$	−2.9	−3.0	−3.5	−3.9
$C_2N_3C_3H_3$	−18.8	−10.8	−4.4	0.12
$C_2N_5'C_5'H_3$	18.8	10.8	4.4	−0.17

[a] CB[8] shows an elliptical cavity with minimum and maximum O−O distances between oxygens lying opposite in the rim being 10.04 and 10.56 Å, respectively. [b] Distance between two oxygens in adjacent glycouril units ranges from 2.377 to 2.396 Å. [c] Distance between the O_1 and H_3 is 3.91−3.97 Å.

was then mapped by examining eigenvalues of Hessian matrix at the point where the gradient of $V(r)$ vanishes, and the critical points (CPs) were thereby located using the program code written in our laboratory.[83] The CPs are characterized in terms of an ordered pair (R, σ), where R and σ denote the rank and signature (the sum of algebraic signs of the eigenvalues) of the Hessian matrix, respectively. These CPs fall into three categories, viz., (3, +3), (3, +1), and (3, −1). The (3, +3) CPs correspond to the local minima and represent potential binding sites for electrophilic interactions in their environs, whereas (3, +1) and (3, −1) refer to the saddle points. A versatile package UNIVIS-2000 was used for visualization of the MESP topography and isosurfaces.[84] NMR chemical shifts (δ) were calculated by subtracting the nuclear magnetic shielding tensors of protons in FC and CB[*n*] from those in the tetramethylsilane (as a reference) using the gauge-independent atomic orbital method.[85] Effect of solvation on the energies and the proton chemical shift (δ_H) values in CB[*n*] complexes were modeled through the self-consistent reaction field (SCRF) theory calculations incorporating the polarizable continuum model[86] implemented in Gaussian 03.

Results and Discussion

CB[*n*] Homologues. ***Energetic and Electronic Structures.*** The atomic numbering schemes in the monomer unit of CB[*n*] and FC are shown in Figure 1. Both the top and side views of the B3LYP/6-31G(d)-optimized CB[*n*] geometries superimposed over their crystal structures are displayed in Figure 2. The pink atoms belong to the crystal structure. As is evident, CB[*n*] analogues emerge with cavities of different sizes, and notably, the diameter of CB[8] is nearly twice that of CB[5]. Stabilization energy of CB[*n*] can be calculated from the unit energy as described in the preceding section. These stabilization energies predict CB[7] to be 22.0 kJ mol^{-1} higher in energy relative to its acyclic polymer devoid of ring strain and large electrostatic repulsions due to ureido oxygens. Furthermore, a destabilization amounting to 31.1 kJ mol^{-1} was predicted for CB[6] at the B3LYP/6-31G(d) level of theory. The homologues with $n = 5$ and 8 are highly unstable; their stabilization energies are 58.8 and 48.8 kJ mol^{-1}, respectively. Thus, the calculated stabilization energies have a hierarchy: CB[7] > CB[6] > CB[8] > CB[5].

Geometrical parameters of CB[*n*] hosts are reported in Table 1. As may be noticed readily, the C═O and C−N bond distances remain unchanged in the CB[5] to CB[8] homologues. A largest contraction of 0.007 Å in the C_4-C_4' bonds was noticed in CB[8] as compared to 1.757 Å in CB[5]. Furthermore, C_3H_1 and C_4H_2 bond distances, 1.098 and 1.100 Å in CB[5] respectively, are 0.004 and 0.002 Å longer in CB[8], while the C_3H_3 bond directed toward carbonyl groups in the CB[*n*] portal is unchanged along the series. A separation between ureido oxygens of adjacent glycouril units in the portal (O_1O_1*) increases from 3.330 Å in CB[5] to 3.942 Å in CB[8]. It may therefore be inferred that the repulsion between ureido oxygens of adjacent glycourils decreases along the series. On the other hand, the distances of oxygen from proton directing toward the portal (O_1H_3) turn out to be 2.425 Å in CB[5] and decrease further to 2.387 Å in CB[8]. The separation of radially opposite ureido oxygens in a portal of CB[8] is 10.30 Å, nearly twice that of CB[5] (5.39 Å). These O−O distances suggest the CB[*n*] portals with $n = 5-7$ are circular, while for CB[8] the portals are slightly elliptical with major and minor axes being 10.56 and 10.04 Å, respectively. It is worth nothing that, when O−O distance in the top portal is the largest, the separation of ureido oxygens in the bottom portal of corresponding glycouril turns out to be minimum and vice versa. Bond angles generally do not vary largely; a largest deviation of 2° was predicted for the angle $C_3N_3C_4$ incorporating ureido group along the CB[*n*] series. From the dihedral angle $O_1C_2N_3C_3$ reported, it may be inferred that the methylene carbon is directed away from the CB[5] cavity as opposed to its orientation in CB[7] or CB[8] hosts wherein it points toward the cavity. For CB[6], the methylene carbon lies in the plane with a marginal deviation of 2°. Stabilization energies calculated for CB[6] turn out to be 9.1 kJ mol^{-1} higher than that for CB[7], but the planarity of $O_1C_2N_3C_4$ (with less angular strain) may partly be responsible for CB[6] as a major product during synthesis of these homologues.[5] A change of 20° for $C_2N_3C_3H_3$ dihedral angle was noticed along the series from CB[5] (−19°) to CB[8] (∼1°). Furthermore, as it is immediately discernible from the superimposed geometries (cf. Figure 2), structures engendered through the B3LYP prescription match very well with those observed from the X-ray data. Various bond distances in the crystal structure are reported in Table 1S in the Supporting Information. It may be inferred that the O_1C_2 bond distance in the crystalline phase of CB[5] (1.219 Å) is assessed very well with the corresponding value of 1.212 Å predicted from the present calculations. Likewise, the O_1C_2 distance, which turns out to be 1.232 Å in the crystalline CB[8] host, is only marginally larger than 1.213 Å predicted. It is further gratifying that the CN distances in these homologues also agree with those obtained from the crystal data: the C_2N_3 bond lengths in the crystal data range from 1.377 Å in CB[5] to 1.368 Å in CB[8], whereas the calculations herein predict it to be 1.393 Å. Furthermore, N_3C_3 and N_3C_4 distances that range from 1.444 to 1.453 Å in the crystal data are predicted to be remarkably close and turn out

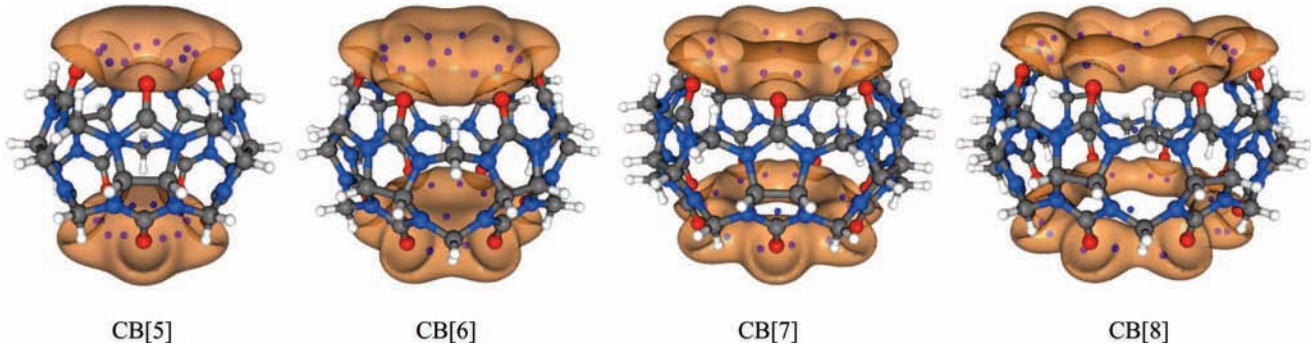

Figure 3. MESP isosurface ($V = -18.4$ kJ mol^{-1}) and CPs in CB[n].

TABLE 2: MESP at the CP and Cavity Dimensions of CB[n]; See Text for Details

	CB[5]	CB[6]	CB[7]	CB[8]
ESP at CP	−299.0	−277.0	−260.5	−250.9
cavity diameter	3.91	5.50	7.11	8.57
cavity height	7.35	7.50	7.63	7.70

to be 1.445−1.447 Å in the present work. Thus, the predicted CB[n] geometries at this level of the theory concur well with the experimental structures.

Bond lengths and bond angles reported in Table 1 are the average of the respective type of bonds in all glycouril monomers. Although the calculations are performed without any symmetry constraints, the predicted bond angles and bond lengths in the CB[n] are practically the same (their deviation being less than 0.002 Å and 0.5°, respectively) in all monomers. Thus, resulting geometries of CB[n], $n = 5-7$, lead naturally to D_{nh} symmetry, while elliptical portals of CB[8] converge with C_{2v} symmetry.

It was already pointed out that the cavity dimension and the charge distribution within the hydrophobic CB[n] cavity primarily governs encapsulation of the guest. MESP brings out the effective localization of the electron-rich regions and thus is expected to provide the molecular level understanding of the host−guest interactions. In the following section we outline the MESP in the CB[n] hosts.

Electrostatic Potential. The molecular electrostatic potential maps give a direct perspective of the segments in the molecules that show affinity toward different types of reactants. A typical MESP isosurface of $V = -18.4$ kJ mol^{-1} in CB[n] homologues is displayed in Figure 3. A negative-valued isosurface encompasses the entire CB[5] portal and is localized near ureido oxygens in portals of CB[8]. Effective cavity dimensions in CB[n] hosts can be estimated from the MESP minima,[87] depicted here as blue dots in the isosurface. The CPs near oxygens in the portal turn out to be coplanar. The MESP minima, cavity height, and cavity diameter at portals of the host are presented in Table 2. The deepest minimum (−299.0 kJ mol^{-1}) is noticed in CB[5] which gradually becomes shallow (−250.9 kJ mol^{-1} in CB[8]) when transverse to higher CB[n] homologues. The "effective cavity diameter", the separation of CPs in the same portal of CB[n] that are radially opposite, was estimated to be 3.91 Å in CB[5] and 8.57 Å in CB[8]. These values are significantly smaller than those derived from the O−O distances within the same portal. Thus, the "effective cavity diameter" in CB[8], on the basis of the MESP topography, is predicted to be 1.73 Å smaller than the separation between the radial opposite oxygens in the portal. Furthermore, the cavity height can be determined from a separation between the two planes incorporating the coplanar MESP minima in the top and bottom portals. The calculated cavity height increases from 7.35 Å in CB[5] to 7.70 Å in CB[8]. The increase in cavity height between two consecutive CB[n] homologues gradually diminishes along the series.

NMR Chemical Shifts. NMR has widely been used as a probe to understand the encapsulation of the guest within the CB[n] cavity; the chemical shifts in the CB[n] hosts have therefore been calculated. Proton chemical shifts (δ_H) in CB[n], $n = 5-8$, observed in gas phase, water, and experiments are compared in Table 3. It is immediately perceived that the methylene proton (H_3) directing toward ureido oxygen is largely deshielded and exhibits a downshift of $\delta_H = 5.9$ ppm, while the other methylene proton (H_1) has its $\delta_H = 3.3$ ppm in the gas-phase spectra, which for H_2 turns out to be 4.6 ppm. These chemical shifts of host protons are not dependent on the number of glycouril units in their isolated state and agree well with those reported by Buschmann et al.[79] In the presence of water as solvent, the δ_H values of H_1, H_2, and H_3 protons in CB[8] turn out to be 3.8, 5.2, and 5.6 ppm, respectively. A separation of NMR signals for H_1 and H_3 in the presence of water predicted here agrees well with that observed in the experimental NMR spectra. Figure 4 depicts the placement of the experimental NMR chemical shifts and compares them with the water-solvated as well as isolated gas-phase values obtained in the present work. A large downshift in δ_H is seen for H_1 and H_2 protons, unlike for the H_3 proton when water is used as solvent. The overall trend of chemical shifts thus obtained is similar to that observed in an experiment and brings out the role of the solvent. Incidentally, the observed δ_H values in CB[n] are seen to be ∼0.4 ppm larger than those obtained from the SCRF calculations.

Inclusion Complexes of Ferrocene and CB[n] Homologues. ***Energetics and Electronic Structures.*** As pointed out earlier, the CB[n] structures for $n = 5-8$ possess cavities in which an appropriate guest molecule could be accommodated, giving a stable inclusion complex. Some inclusion complexes with the FC molecule as a guest with both parallel as well as perpendicular orientations to CB[n] axis of C_n symmetry are displayed in Figure 5. The electronic energy (E), counterpoise corrected energy (CE), and counterpoise basis set superposition error (BSSE) (in hartrees) are reported in Table 4, along with the relative stabilization energies (ΔE an ΔCE both in kilojoules per mole) of the FC−CB[n] complexes. As may be noticed from Table 4, the contributions from the BSSE are relatively very small for the complexes possessing weak host−guest interactions, viz., lateral interactions of guest FC with CB[5] or CB[6] and parallel in CB[7] or CB[8]. The relative stabilization energies further reveal that the perpendicular orientation of FC is preferred over its parallel orientation in the complex with large CB[n] cavities, and the counterpoise corrected energies exhibit a similar trend. The binding energies (ΔE_{bind}), obtained

TABLE 3: NMR Chemical Shifts, δ_H (in Parts per Million) in CB[n] in Gas Phase and in Water

	CB[5]			CB[6]			CB[7]			CB[8]		
	gas phase	water	obsd[a]	gas phase	water	obsd[a]	gas phase	water	obsd[a]	gas phase	water	obsd[a]
H_1	3.3	3.8	4.43	3.2	3.8	4.31	3.2	3.8	4.29	3.2	3.8	4.28
H_2	4.6	5.2	5.65	4.6	5.2	5.59	4.5	5.2	5.60	4.4	5.2	5.60
H_3	5.9	5.5	5.85	6.0	5.6	5.87	6.1	5.6	5.91	6.1	5.6	5.93

[a] Reference 4.

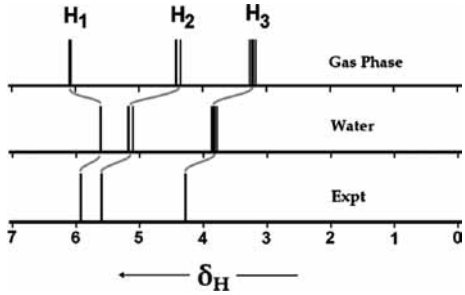

Figure 4. NMR chemical shifts (δ_H) in CB[8] in gas phase and in water compared with those observed experimentally.

by subtracting electronic energy of the complex from the sum of electronic energy of CB[n] and FC individually, are given in Table 5. It may be inferred that the lateral interaction of FC with the hydrophilic exterior of the CB[n] or its encapsulation within the cavity is not favored with CB[5], and in both the cases $\Delta E_{bind} < 0$ suggests destabilization of the complex relative to individual host and guest. Lateral interactions with FC are favored ($\Delta E_{bind} = 12.7$ kJ mol^{-1}) when CB[6] was used as a host, however. Large cavity dimensions in CB[7] or CB[8] allow the guest FC to get encapsulated within the host cavity either parallel or perpendicular to CB[n] symmetry axis. The ΔE_{bind} data in the gas phase predict that the complexes FC(⊥)CB[n] (guest with perpendicular orientation) are favored in both CB[7] (17.1 kJ mol^{-1}) and CB[8] (51.9 kJ mol^{-1}) compared with the binding energies of 4.0 and 34.1 kJ mol^{-1}, respectively, when FC penetrates parallely within the host cavity. Binding energies from the SCRF calculations are reported in Table 6, where the preference for the parallel orientation of FC in CB[7] and CB[8] complexes in the presence of solvent is noticeable. For CB[7] and CB[8], the binding energies of FC(||)CB[n] complexes are lowered by −8.9 and −2.1 kJ mol^{-1} as compared to FC(⊥)CB[n] complex, respectively.

The top and side views of B3LYP-optimized FC(||)CB[7] and FC(⊥)CB[7] structures superimposed on the corresponding X-ray crystal structures are shown in Figure 1S in the Supporting Information. Crystal structures of inclusion complexes showing parallel and perpendicular orientations of FC within CB[7] are reported in ref 12. The figure is self-evident that predicted geometries of these complexes agree well with the crystal structures. Thus, in FC(||)CB[7], inclination of guest with an angle of 29° with the CB[7] axis is predicted when FC penetrates along the host cavity, while the crystal data of the same shows FC inclined with 22°. On the other hand, when FC penetrates perpendicular to the CB[7] cavity the guest is inclined at an angle of 86° (compared to 79° in crystal structure). Distances from the center of FC (i.e., Fe) from O_1 as well as C_4 are as follows: the average FeO_1 distance predicted from the present calculations turns out to be 5.27 and 5.25 Å in FC(||)CB[7] and FC(⊥)CB[7], respectively, compared to 5.39 Å in the X-ray data for both complexes. Furthermore, the calculated FeC_4 distance in both the complexes turns out to be 5.85 Å, which has been observed to be 5.89 Å in the crystal. In addition, a structure with FC molecule inclined at 84° with the cavity axis was obtained when CB[8] was used as a host. An encapsulation of FC in CB[8] thus engenders an inclusion complex possessing two equivalent portals with the guest practically oriented along the cavity axis (deviation only within 1°).

Electrostatic Potentials. MESP isosurfaces in FC and FC(X)−CB[n] (where X refers to the lateral, parallel, and perpendicular orientation of guest; i.e., L, ||, and ⊥, respectively) complexes are shown in Figure 2S in the Supporting Information. Aromatic π-electrons of cyclopentadiene ring engender a negative-valued MESP region in FC. Thus, the repulsions arising from these electron-rich regions of the guest with highly negative portal caused by carbonyl oxygens partly explain why lateral interaction of FC with the CB[5] host leads to a destabilized FC(L)CB[5] complex.

NMR Chemical Shifts in FC−CB[n] Inclusion Complexes. NMR spectra of FC and inclusion complexes with the CB[7] and CB[8] are compared in Figure 6. The δ_H values in the inclusion complexes are given in Table 2S in the Supporting Information. The dependence of δ_H values on the parallel or perpendicular orientation of the guest (FC) in these complexes is interpreted as follows. On encapsulation, the FC protons are shielded to a greater extent in the FC(⊥)CB[n] complex and an average upshift turns out to be 3.45 ppm for the CB[7] inclusion complex. As pointed out earlier, FC is tilted in the CB[7] cavity, which results in different δ_H values for guest protons in the NMR spectra. As shown in Figure 6, the FC signals in this complex appear from $\delta_H = 3.30$ to 3.91 ppm. A proton located midway between nitrogens of adjacent glycouril units is predicted at $\delta_H = 3.41$ ppm, while those pointing toward the portal downshift to $\delta_H = 3.70$ ppm. Thus, FC protons, which interact with portal oxygen, exhibit large δ_H values. An NMR signal at $\delta_H = 3.32$ ppm was predicted when the guest penetrates the CB[8] cavity axis. Parallel orientation of FC engenders a structure with equivalent portals with the guest fitting linearly. For perpendicular FC orientation, the unsymmetrical environment for FC proton in the complex results from the interaction of different number of oxygens in each portal with FC (cf. Figure 5). For FC(⊥)CB[n] complexes, NMR signals of guest protons are seen to be relatively complex and yield different δ_H values ranging from 3.30 to 3.91 ppm in the FC(⊥)CB[7] complex. Here, the protons, which interact with nitrogens, are associated with $\delta_H = 3.57$ ppm and those pointing toward one of the portals show up at a relatively large δ_H value (3.79 ppm). Thus, the protons interacting with the portal oxygens are essentially deshielded to a greater extent as compared to those in the isolated guest. As noticed earlier, the FC protons in the FC(⊥)CB[8] complex appear in the range $\delta_H = 3.34-3.74$ ppm. A comparison of the NMR spectra of these complexes with corresponding CB[n] hosts led to the following inferences. A downshift in the proton signals can be noticed in the complexes possessing parallel orientation of FC. Encapsulation of FC within the CB[7] cavity leads to closely spaced NMR signals of H_1 protons ranging, viz., $\delta_H = 3.25-3.40$ ppm when FC is parallel to the CB[7] cavity. Widely spaced NMR signals for these protons ($\delta_H = 2.98-3.36$ ppm) are noticed when the guest

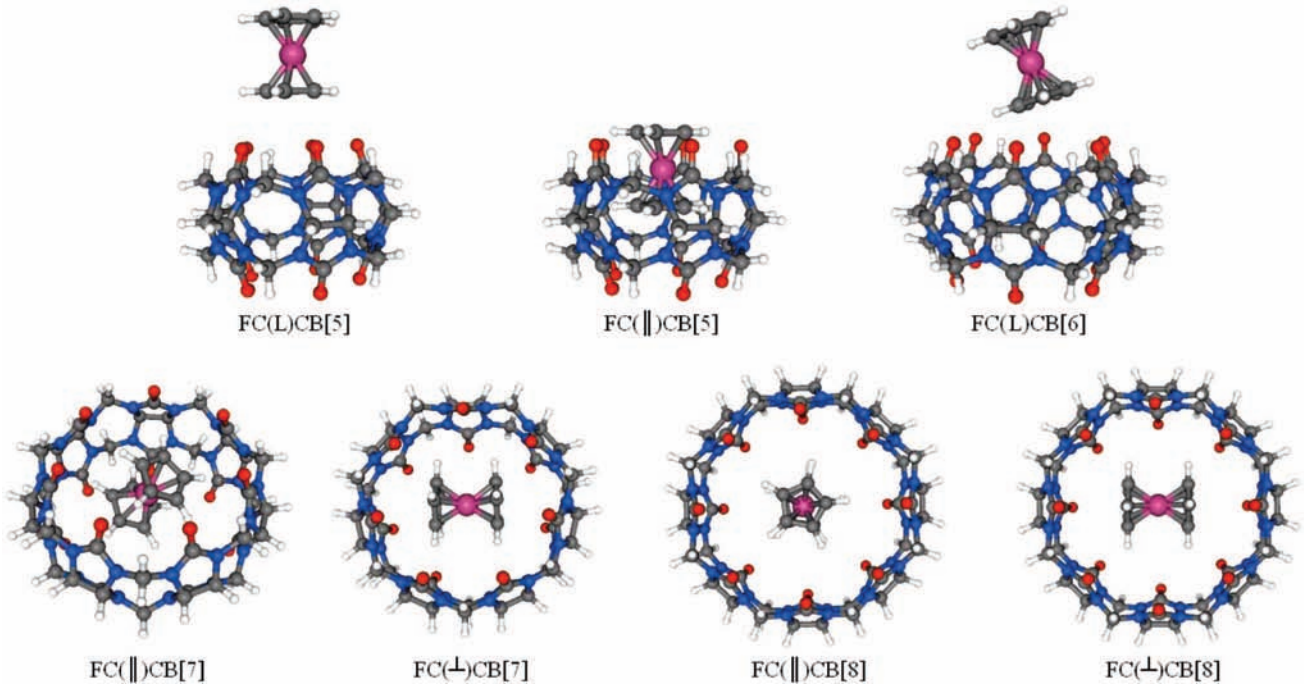

Figure 5. Optimized geometries for FC−CB[*n*] complexes.

TABLE 4: Electronic Energy (*E*), Counterpoise Corrected Energy (*CE*), Counterpoise BSSE Energy (in Hartrees), and Relative Stabilization Energies (Δ*E* and Δ*CE* Both in Kilojoules per Mole) of the FC−CB[*n*] Complexes

			counterpoise		
	E	Δ*E*	*CE*	Δ*CE*	BSSE energy
FC(‖)CB[5]	−4659.2539	477.74	−4659.2272	530.43	0.026702
FC(L)CB[5]	−4659.4359	0.00	−4659.4292	0.00	0.006518
FC(L)CB[6]	−5261.2047	0.00	−5261.1895	0.00	0.007986
FC(‖)CB[7]	−5862.9562	13.09	−5862.9378	8.89	0.014236
FC(⊥)CB[7]	−5862.9612	0.00	−5862.9412	0.00	0.019165
FC(‖)CB[8]	−6464.7090	17.70	−6464.7025	9.33	0.006008
FC(⊥)CB[8]	−6464.7157	0.00	−6464.7060	0.00	0.009438

TABLE 5: Binding Energies (ΔE_{bind}) (in Kilojoules per Mole) of FC−CB[*n*] Complexes

	ΔE_{bind}		
	L	‖	⊥
FC−CB[5]	−5.2	−483.0	
FC−CB[6]	12.7		
FC−CB[7]		4.0	17.1
FC−CB[8]		34.1	51.9

TABLE 6: Binding Energies (in Kilojoules per Mole) of FC−CB[*n*] Complexes in Water

	ΔE_{bind}	
	‖	⊥
FC−CB[7]	−12.4	−21.3
FC−CB[8]	−1.0	−3.1

oriented perpendicular to the CB[7] axis. The predicted δ_H values in CB[7] exhibit a larger separation since the guest is tilted within the CB[*n*] cavity leading to an unsymmetrical environment. When the guest is placed parallel to CB[8], H_1 protons yield closely spaced NMR signals around $\delta_H = 3.29$ ppm. On the other hand, perpendicular penetration of guest in CB[8] leads to a number of NMR signals between $\delta_H = 3.02$ and 3.30 ppm. Similar inferences can be drawn for H_2 and H_3 protons as well in both CB[7] and CB[8] inclusion complexes.

The FC protons in gaseous state show at $\delta_H = 3.62$ ppm which are downshifted to $\delta_H = 3.88$ ppm in the presence of water as solvent. It should be further noticed that on solvation these protons in the FC(‖)CB[*n*] complex get more shielded. When the guest orients in a perpendicular fashion, the NMR signals are downshifted further and are closely spaced as shown in Figure 6. In the gas phase, these FC protons in the FC(⊥)CB[8] complex are predicted between $\delta_H = 3.34-3.74$ ppm; a separation of 0.40 ppm has thus been noted. The solvent reduces such a separation to 0.21 ppm ($\delta_H = 3.39-3.60$ ppm). Similar conclusions could be drawn when FC orients perpendicular to the CB[7] cavity in the presence of water. On the other hand, relatively sparsely spaced NMR signals are noticed for the parallel orientation. The upshifted signals can also be seen in the case of the FC(‖)CB[8] complex. Calculated NMR spectra in these inclusion complexes establish that on solvation H_1 and H_2 protons are downshifted, whereas the H_3 proton exhibits a shift in opposite direction as noticed earlier in case of isolated CB[*n*] hosts. The NMR spectra with average chemical shifts of protons in CB[*n*] (*n* = 7, 8), FC, and their complexes with water as a solvent are compared in Figure 3S in the Supporting Information. Complexes having a parallel orientation of the guest lead invariably to a relatively large upshift for the FC protons compared to those possessing perpendicular orientation of the guest in the complex. On the other hand, CB[*n*] protons show a downshift in the NMR in former host−guest complexes.

Conclusions

Systematic ab initio investigations of electronic structure, MESP, and NMR chemical shifts in the CB[*n*], FC, and their complexes were carried out at the B3LYP/6-31G(d) level of theory. The following conclusions may be drawn. (i) Calculated stabilization energies subscribe to a hierarchy as CB[7] > CB[6] > CB[8] > CB[5]. The O_1-O_1 distances between the adjacent glycouril units suggest the repulsions between ureido groups decrease along CB[*n*] homologue series. (ii) The lower homologue CB[5] does not favor interaction with FC and does not

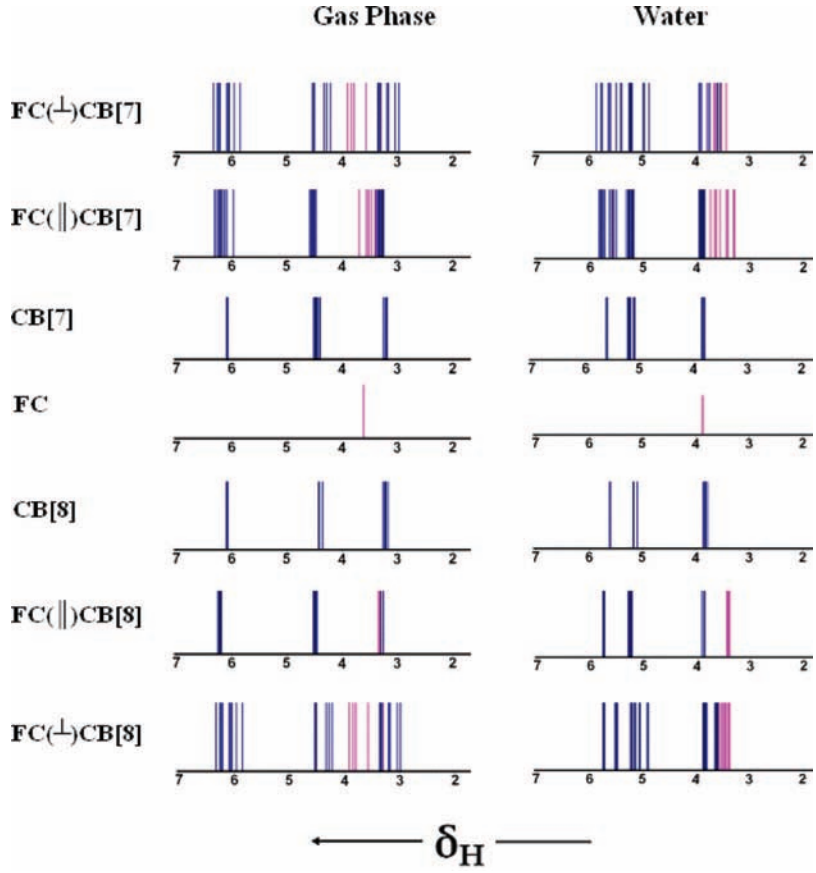

Figure 6. Chemical shifts in FC, CB[*n*], $n = 7$ and 8, and their inclusion complexes in gas phase and water.

yield any stable structure. Both CB[7] and CB[8] on the other hand lead to inclusion complexes with the guest FC being accommodated within the cavity in parallel as well as perpendicular orientation relative to the CB[*n*] axis. The electronic structure and the geometrical parameters of the FC−CB[7] complex thus derived agree well with the X-ray crystal data. A structure of the complex with FC perpendicular to cavity axis is seen to be favored in the gas phase; however, aqueous solvation prefers parallel orientation of the guest. (iii) NMR spectra of the CB[*n*] homologues are similar and the δ_H values of respective protons remain unchanged on going from CB[5] to CB[8]. SCRF calculations reveal that solvation with water influences chemical shifts significantly, and the resulting spectra are in accordance with the experiments. (iv) FC protons in the inclusion complexes of CB[7] or CB[8] directed toward the portals get deshielded more and hence have a δ_H downshift while those pointing between nitrogens of glycourils exhibit an upshift in δ_H relative to the gas-phase values. (v) The orientation of FC in CB[7] or CB[8] inclusion complexes has a significant influence on NMR spectra: the δ_H values of host and guest protons are relatively closely placed when the FC orients parallel to the CB[*n*] axis. Calculated spectra further reveal that NMR signals in the presence of water as solvent occur in a narrower span for a perpendicular orientation of the guest to the CB[*n*] axis, unlike its parallel orientation in CB[7].

Acknowledgment. We thank the Center for Network Computing, University of Pune, for providing computational facilities and Professor R. K. Pathak for useful discussions. S.P.G. is grateful to the University Grants Commission, New Delhi, India (Research Project F30-72/2004(SR)) and University of Pune for disbursing the research grant under the potential excellence scheme. R.V.P. acknowledges the Council of Scientific and Industrial Research for a senior research fellowship.

Supporting Information Available: Bond distances in the crystal structure of CB[*n*] homologues, views of the B3LYP geometries superimposed on the crystal structure of inclusion complexes, electrostatic potentials in FC−CB[*n*] complexes, chemicals shifts of protons in FC−CB[*n*], $n = 7$, 8, complexes and comparison of average chemical shifts of their protons in gas phase and water. This material is available free of charge via the Internet at http://pubs.acs.org.

References and Notes

(1) Lagona, J.; Mukhopadhyay, P.; Chakrabarti, S.; Isaacs, L. *Angew. Chem., Int. Ed.* **2005**, *44*, 4844.
(2) Freeman, W. A.; Mock, W. L.; Shih, N.-Y. *J. Am. Chem. Soc.* **1981**, *103*, 7367.
(3) Behrend, R.; Meyer, E.; Rusche, F. *Justus Liebigs Ann. Chem.* **1905**, *339*, 1.
(4) Kim, J.; Jung, I.-S.; Kim, S.-Y.; Lee, E.; Kang, J.-K.; Sakamoto, S.; Yamaguchi, K.; Kim, K. *J. Am. Chem. Soc.* **2000**, *122*, 540.
(5) Day, A. I.; Arnold, A. P.; Blanch, R. J.; Snushall, B. *J. Org. Chem.* **2001**, *66*, 8094.
(6) Buschmann, H.-J.; Jansen, K.; Schollmeyer, E. *Thermochim. Acta* **1998**, *317*, 95.
(7) Buschmann, H.-J.; Jansen, K.; Schollmeyer, E. *Thermochim. Acta* **2000**, *346*, 33.
(8) Buschmann, H.-J.; Schollmeyer, E.; Mutihac, L. *Thermochim. Acta* **2003**, *399*, 203.
(9) Heitmann, L. M.; Taylor, A. B.; Hart, P. J.; Urbach, A. R. *J. Am. Chem. Soc.* **2006**, *128*, 12574.
(10) Lee, J. W.; Samal, S.; Selvapalam, N.; Kim, H.-J.; Kim, K. *Acc. Chem. Res.* **2003**, *36*, 621.
(11) Ong, W.; Kaifer, A. E. *Organometallics* **2003**, *22*, 4181.
(12) Jeon, W. S.; Moon, K.; Park, S. H.; Chun, H.; Ko, Y. H.; Lee, J. Y.; Lee, E. S.; Samal, S.; Selvapalam, N.; Rekharsky, M. V.; Sindelar,

V.; Sobransingh, D.; Inoue, Y.; Kaifer, A. E.; Kim, K. *J. Am. Chem. Soc.* **2005**, *127*, 12984.
(13) Feng, K.; Wu, L.-Z.; Zhang, L.-P.; Tung, C.-H. *Dalton Trans.* **2007**, 3991.
(14) Wheate, N. J.; Taleb, R. I.; Krause-Heuer, A. M.; Cook, R. L.; Wang, S.; Higgins, V. J.; Aldrich-Wright, J. R. *Dalton Trans.* **2007**, 5055.
(15) Sobransingh, D.; Kaifer, A. E. *Langmuir* **2006**, *22*, 10540.
(16) Lorenzo, S.; Day, A.; Craig, D.; Blanch, R.; Arnold, A.; Dance, I. *CrystEngComm* **2001**, *49*, 1.
(17) Buschmann, H.-J.; Jansen, K.; Schollmeyer, E. *Inorg. Chem. Commun.* **2003**, *6*, 531.
(18) Wheate, N. J.; Buck, D. P.; Day, A. I.; Collins, J. G. *Dalton Trans.* **2006**, 451.
(19) Bali, M. S.; Buck, D. P.; Coe, A. J.; Day, A. I.; Collins, J. G. *Dalton Trans.* **2006**, 5337.
(20) Zhang, X. X.; Krakowiak, K. E.; Xue, G.; Bradshaw, J. S.; Izatt, R. M. *Ind. Eng. Chem. Res.* **2000**, *39*, 3516.
(21) Gerasko, O. A.; Mainicheva, E. A.; Naumova, M. I.; Yurjeva, O. P.; Alberola, A.; Vicent, C.; Llusar, R.; Fedin, V. P. *Eur. J. Inorg. Chem.* **2008**, 416.
(22) Buschmann, H.-J.; Jansen, K.; Meschke, C.; Schollmeyer, E. *J. Solution Chem.* **1998**, *27*, 135.
(23) Izatt, R. M.; Terry, R. E.; Haymore, B. L.; Hansen, L. D.; Dalley, N. K.; Avondet, A. G.; Christensen, J. J. *J. Am. Chem. Soc.* **1976**, *98*, 7620.
(24) Jansen, K.; Buschmann, H.-J.; Wego, A.; Döpp, D.; Mayer, C.; Drexler, H. J.; Holdt, H. J.; Schollmeyer, E. *J. Inclusion Phenom. Macrocyclic Chem.* **2001**, *39*, 357.
(25) Wei, F.; Liu, S.-M.; Xu, L.; Cheng, G.-Z.; Wu, C.-T.; Feng, Y.-Q. *Electrophoresis* **2005**, *26*, 2214.
(26) Xu, L.; Liu, S.-M.; Wu, C.-T.; Feng, Y.-Q. *Electrophoresis* **2004**, *25*, 3300.
(27) Mock, W. L. *Top. Curr. Chem.* **1995**, *175*, 1.
(28) Hoffmann, R.; Knoche, W.; Fenn, C.; Buschmann, H.-J. *J. Chem. Soc., Faraday Trans.* **1994**, *90*, 1507.
(29) Kim, K. *Chem. Soc. Rev.* **2002**, *31*, 96.
(30) Lehn, J.-M. *Angew. Chem., Int. Ed.* **1988**, *27*, 89.
(31) Cram, D. J. *Angew. Chem., Int. Ed.* **1988**, *27*, 1009.
(32) Pedersen, C. J. *Angew. Chem., Int. Ed.* **1988**, *27*, 1021.
(33) Jeon, Y. J.; Bharadwaj, P. K.; Choi, S. W.; Lee, J. W.; Kim, K. *Angew. Chem., Int. Ed.* **2002**, *41*, 4474.
(34) Rauwald, U.; Scherman, O. A. *Angew. Chem., Int. Ed.* **2008**, *47*, 3950.
(35) Sindelar, V.; Cejas, M. A.; Raymo, F. M.; Chen, W.; Parker, S. E.; Kaifer, A. E. *Chem.−Eur. J.* **2005**, *11*, 7054.
(36) Ko, Y. H.; Kim, E.; Hwang, I.; Kim, K. *Chem. Commun.* **2007**, 1305.
(37) Mohanty, J.; Pal, H.; Ray, A. K.; Kumar, S.; Nau, W. M. *Chem. Phys. Chem.* **2007**, *8*, 54.
(38) Kolb, H. C.; Finn, M. G.; Sharpless, K. B. *Angew. Chem., Int. Ed.* **2001**, *40*, 2004.
(39) Tuncel, D.; Steinke, J. H. G. *Macromolecules* **2004**, *37*, 288.
(40) Tuncel, D.; Steinke, J. H. G. *Chem. Commun.* **2002**, 496.
(41) Mukhopadhyay, P.; Wu, A.; Isaacs, L. *J. Org. Chem.* **2004**, *69*, 6157.
(42) Burnett, C. A.; Witt, D.; Fettinger, J. C.; Isaacs, L. *J. Org. Chem.* **2003**, *68*, 6184.
(43) Wheate, N. J.; Day, A. I.; Blanch, R. J.; Arnold, A. P.; Cullinane, C.; Collins, J. G. *Chem. Commun.* **2004**, 1424.
(44) Isobe, H.; Tomita, N.; Lee, J. W.; Kim, H.-J.; Kim, K.; Nakamura, E. *Angew. Chem., Int. Ed.* **2000**, *39*, 4257.
(45) Lim, Y.-B.; Kim, T.; Lee, J. W.; Kim, S.-M.; Kim, H.-J.; Kim, K.; Park, J.-S. *Bioconjugate Chem.* **2002**, *13*, 1181.
(46) Balzani, V.; Credi, A.; Raymo, F. M.; Stoddart, J. F. *Angew. Chem., Int. Ed.* **2000**, *39*, 3348.
(47) Corma, A.; García, H.; Montes-Navajas, P.; Primo, A.; Calvino, J. J.; Trasobares, S. *Chem.−Eur. J.* **2007**, *13*, 6359.
(48) Sobransingh, D.; Kaifer, A. E. *Chem. Commun.* **2005**, 5071.
(49) Roh, S.-G.; Park, K.-M.; Park, G.-J.; Sakamoto, S.; Yamaguchi, K.; Kim, K. *Angew. Chem., Int. Ed.* **1999**, *38*, 638.
(50) Park, K.-M.; Kim, S.-Y.; Heo, J.; Whang, D.; Sakamoto, S.; Yamaguchi, K.; Kim, K. *J. Am. Chem. Soc.* **2002**, *124*, 2140.
(51) Ko, Y. H.; Kim, K.; Kang, J.-K.; Chun, H.; Lee, J. W.; Sakamoto, S.; Yamaguchi, K.; Fettinger, J. C.; Kim, K. *J. Am. Chem. Soc.* **2004**, *126*, 1932.
(52) Mock, W. L.; Irra, T. A.; Wepsiec, J. P.; Adhya, M. *J. Org. Chem.* **1989**, *54*, 5302.
(53) Meschke, C.; Buschmann, H.-J.; Schollmeyer, E. *Macromol. Rapid Commun.* **1998**, *19*, 59.
(54) Liu, S.-M.; Wu, X.; Huang, Z.; Yao, J.; Liang, F.; Wu, C.-T. *J. Inclusion Phenom. Macrocyclic Chem.* **2004**, *50*, 203.
(55) He, X.; Li, G.; Chen, H. *Inorg. Chem. Commun.* **2002**, *5*, 633.
(56) Lee, E.; Heo, J.; Kim, K. *Angew. Chem., Int. Ed.* **2000**, *39*, 2699.
(57) Lee, E.; Kim, J.; Heo, J.; Whang, D.; Kim, K. *Angew. Chem., Int. Ed.* **2001**, *40*, 399.
(58) Park, K.-M.; Roh, S.-G.; Lee, E.; Kim, J.; Kim, H.-J.; Lee, J. W.; Kim, K. *Supramol. Chem.* **2002**, *14*, 153.
(59) Park, K.-M.; Whang, D.; Lee, E.; Heo, J.; Kim, K. *Chem.−Eur. J.* **2002**, *8*, 498.
(60) Liu, J.; Xu, Y.; Li, X.; Tian, H. *Dyes Pigm.* **2008**, *76*, 294.
(61) Zhao, M.; Wang, Z.-B.; Li, Y.-Z.; Chen, H.-L. *Inorg. Chem. Commun.* **2007**, *10*, 101.
(62) Marquez, C.; Nau, W. M. *Angew. Chem., Int. Ed.* **2001**, *40*, 3155.
(63) Jon, S. Y.; Ko, Y. H.; Park, S. H.; Kim, H.-J.; Kim, K. *Chem. Commun.* **2001**, 1938.
(64) Lee, J. W.; Kim, K.; Choi, S.; Ko, Y. H.; Sakamoto, S.; Yamaguchi, K.; Kim, K. *Chem. Commun.* **2002**, 2692.
(65) Wang, R.; Yuan, L.; Macartney, D. H. *J. Org. Chem.* **2006**, *71*, 1237.
(66) Wu, X.-L.; Luo, L.; Lei, L.; Liao, G.-H.; Wu, L.-Z.; Tung, C.-H. *J. Org. Chem.* **2008**, *73*, 491.
(67) Pattabiraman, M.; Kaanumalle, L. S.; Natarajan, A.; Ramamurthy, V. *Langmuir* **2006**, *22*, 7605.
(68) Maddipatla, M. V. S. N.; Kaanumalle, L. S.; Natarajan, A.; Pattabiraman, M.; Ramamurthy, V. *Langmuir* **2007**, *23*, 7545.
(69) Lei, L.; Luo, L.; Wu, X.-L.; Liao, G.-H.; Wu, L.-Z.; Tung, C.-H. *Tetrahedron Lett.* **2008**, *49*, 1502.
(70) Kim, H.-J.; Heo, J.; Jeon, W. S.; Lee, E.; Kim, J.; Sakamoto, S.; Yamaguchi, K.; Kim, K. *Angew. Chem., Int. Ed.* **2001**, *40*, 1526.
(71) Zou, D.; Andersson, S.; Zhang, R.; Sun, S.; Åkermark, B.; Sun, L. *J. Org. Chem.* **2008**, *73*, 3775.
(72) Ong, W.; Kaifer, A. E. *Angew. Chem., Int. Ed.* **2003**, *42*, 2164.
(73) Sobransingh, D.; Kaifer, A. E. *Chem. Commun.* **2005**, 5071.
(74) Oh, K. S.; Yoon, J.; Kim, K. S. *J. Phys. Chem. B* **2001**, *105*, 9726.
(75) Pichierri, F. *J. Mol. Struct.: THEOCHEM* **2006**, *765*, 151.
(76) Pichierri, F. *Chem. Phys. Lett.* **2004**, *390*, 214.
(77) Carlqvist, P.; Maseras, F. *Chem. Commun.* **2007**, 748.
(78) Pichierri, F. *Chem. Phys. Lett.* **2005**, *403*, 252.
(79) Buschmann, H.-J.; Wego, A.; Zielesny, A.; Schollmeyer, E. *J. Inclusion Phenom. Macrocyclic Chem.* **2006**, *54*, 241.
(80) Frisch, M. J.; Trucks, G. W.; Schlegel, H. B.; Scuseria, G. E.; Robb, M. A.; Cheeseman, J. R.; Montgomery, J. A., Jr.; Vreven, T.; Kudin, K. N.; Burant, J. C.; Millam, J. M.; Iyengar, S. S.; Tomasi, J.; Barone, V.; Mennucci, B.; Cossi, M.; Scalmani, G.; Rega, N.; Petersson, G. A.; Nakatsuji, H.; Hada, M.; Ehara, M.; Toyota, K.; Fukuda, R.; Hasegawa, J.; Ishida, M.; Nakajima, T.; Honda, Y.; Kitao, O.; Nakai, H.; Klene, M.; Li, X.; Knox, J. E.; Hratchian, H. P.; Cross, J. B.; Bakken, V.; Adamo, C.; Jaramillo, J.; Gomperts, R.; Stratmann, R. E.; Yazyev, O.; Austin, A. J.; Cammi, R.; Pomelli, C.; Ochterski, J. W.; Ayala, P. Y.; Morokuma, K.; Voth, G. A.; Salvador, P.; Dannenberg, J. J.; Zakrzewski, V. G.; Dapprich, S.; Daniels, A. D.; Strain, M. C.; Farkas, O.; Malick, D. K.; Rabuck, A. D.; Raghavachari, K.; Foresman, J. B.; Ortiz, J. V.; Cui, Q.; Baboul, A. G.; Clifford, S.; Cioslowski, J.; Stefanov, B. B.; Liu, G.; Liashenko, A.; Piskorz, P.; Komaromi, I.; Martin, R. L.; Fox, D. J.; Keith, T.; Al-Laham, M. A.; Peng, C. Y.; Nanayakkara, A.; Challacombe, M.; Gill, P. M. W.; Johnson, B.; Chen, W.; Wong, M. W.; Gonzalez, C.; Pople, J. A. Gaussian 03, revision C.02; Gaussian, Inc.: Wallingford, CT, 2004.
(81) Becke, A. D. *Phys. Rev. A* **1988**, *38*, 3098.
(82) Lee, C.; Yang, W.; Parr, R. G. *Phys. Rev. B* **1988**, *37*, 785.
(83) Balanarayan, P.; Gadre, S. R. *J. Chem. Phys.* **2003**, *119*, 5037.
(84) Limaye, A. C.; Gadre, S. R. *Curr. Sci.* **2001**, *80*, 1298.
(85) Wolinski, K.; Hilton, J. F.; Pulay, P. *J. Am. Chem. Soc.* **1990**, *112*, 8251.
(86) Miertš, S.; Scrocco, E.; Tomasi, J. *Chem. Phys.* **1981**, *55*, 117.
(87) Pinjari, R. V.; Joshi, K. A.; Gejji, S. P. *J. Phys. Chem. A* **2006**, *110*, 13073.

JP807268V